Pion-nucleon partial-wave amplitudes

R. E. Cutkosky, C. P. Forsyth, and R. E. Hendrick*
Carnegie-Mellon University, Pittsburgh, Pennsylvania 15213

R. L. Kelly
Lawrence Berkeley Laboratory, Berkeley, California 94720
(Received 29 May 1979)

We report pion-nucleon partial-wave amplitudes obtained from analysis of scattering data at pion laboratory momenta from 0.42 to 2.0 GeV/c. These partial-wave amplitudes have been analyzed using modified Breit-Wigner, coupled-channel parametrizations. The resulting resonances and their parameters are tabulated.

I. INTRODUCTION

For over two decades it has been clear that baryons are not simple particles. The emerging picture of a baryon is a system of three quarks bound together by colored gluonic forces. Excitations of baryons in this picture correspond to flavor excitations of the constituent quarks or orbital excitations among the quarks and gluons. Such excitations give rise to the full baryon spectrum. A better knowledge of the baryon spectrum is essential to testing this picture, or any other picture, of the baryon. Detailed information about excited states of baryons gives a critical proving-ground for dynamical models of the baryon and provides another set of constraints on any fundamental theory of strong interactions.

In this paper we give results on the segment of the baryon spectrum accessible through pion-nucleon scattering: uncharged and doubly charged baryon states with strangeness zero. The preceding paper[1] described a partial-wave analysis of pion-nucleon scattering at laboratory momenta between 0.42 and 2.0 GeV/c. In the first step of the analysis, amalgamated differential-cross-section and polarization data were prepared at convenient values of momenta, using techniques presented in an accompanying paper.[2] At each of these momenta, the partial-wave analyses used an accelerated-convergence expansion for efficient representation of the scattering amplitude. Hyperbolic-dispersion-relation techniques were used to resolve ambiguities in accordance with s-channel analyticity. The analysis resulted in $I=\frac{1}{2}$ and $I=\frac{3}{2}$ partial waves for angular momenta through $J=\frac{39}{2}$ in the prescribed energy range.

This paper presents the nonperipheral partial wave amplitudes and discusses those amplitudes in terms of their resonant structure. Each partial wave has been parametrized using a smoothly varying background term along with modified Breit-Wigner resonance terms as required. The standard Breit-Wigner resonance form has been modified to include energy-dependent phase-space factors for the πN elastic channel, quasi-two-body channels such as $\pi\Delta$, ρN, ηN, ϵN, ωN, πN^*, and $\rho\Delta$, and a nonresonant three-body $\pi\pi N$ channel. Our parametrization of partial-wave amplitudes refers to a multichannel scattering matrix which includes couplings among several inelastic channels. In practice, explicit parametrization of multichannel couplings becomes important when several resonances occur at nearby energies in a single partial wave, or when an important channel opens within the width of a resonance.

The potentials included in our formalism are chosen to give our elastic partial-wave parametrizations the correct analyticity structure. An isobar model is used to parametrize inelastic channels. As an additional constraint, we require our partial-wave parametrizations to be in general agreement with isobar production cross sections determined by SLAC-Berkeley[3] and Imperial College[4] partial-wave analyses of single-pion production data. This is done by fitting our partial-wave parametrizations to the determined inelastic cross sections as well as to the elastic partial-wave amplitudes.

A number of analyses of resonances in pion-nucleon scattering have been reported in the literature. The recent Helsinki-Karlsruhe[5] analysis (referred to hereafter as HK) makes use of fixed-t dispersion relations to arrive at partial-wave amplitudes. Earlier analyses by Ayed,[6] Almehed and Lovelace,[7] and Davies[8] have reported resonance parameters over a similar energy range. These analyses, Refs. 6–8, did not include some of the more recent charge-exchange cross-section and polarization data, and have used a number of

alternative methods to eliminate ambiguities and include analyticity constraints. Several analyses have reported results at lower energies, including a recent analysis by Zidell *et al.*[9] and a reanalysis of low-energy data by Bugg.[10]

Results from an earlier stage of the present analysis have been previously reported.[11] The present results include new data and cover a larger energy range. The method of partial-wave resonance parametrization is also substantially changed.

Section II of this paper gives a detailed description of our partial-wave parametrizations, including a discussion of the channel-coupling formalism and phase-space factors. Our definitions of resonance parameters are presented and discussed in Sec. III. In Sec. IV we present figures showing all partial-wave amplitudes in which we find resonances. Several partial waves, including P_{11}, P_{31}, P_{13}, F_{15}, and G_{17}, have subtle structure which is difficult to resolve. In each of these partial waves, parametrizations with additional resonances have been found. Careful further analysis of the statistical confidence level of these additional states and of possible systematic biases is required before a final accounting can be given. Thus, we report only the more definite resonances and their parameters in Sec. IV. We summarize our results and compare them with other recent work in Sec. V.

II. PARTIAL-WAVE PARAMETRIZATION

The structure in individual partial waves is the key to resonant states of the baryon. To unravel that structure, partial-wave parametrizations must have the appropriate partial-wave analyticity, accommodate a smoothly varying background without introducing artificial resonant structure, and be able to fit a number of closely spaced resonances.

Standard elastic partial-wave analyses restrict their parametrizations to the elastic amplitude. Our analysis attempts to extend the parametrization to include coupling of the elastic channel to various inelastic channels. This is done by extending the dimensions of the scattering matrix, including potentials which connect the elastic channel to appropriate inelastic channels. Rather than discussing only the elastic transition amplitude, we parametrize the t matrix [see Fig. 1(a)] to be

$$t_{ab}=\gamma_{ia}f_a(s)G_{ij}\gamma_{jb}f_b(s)\,, \tag{2.1}$$

where $a(b)$ represents the outgoing (incoming) channel $a=1,\ldots,M$, including the elastic channel. Initial and final channels couple through intermediate "particles" or resonances, labeled by $i,j=1,\ldots,N$. The factors γ_{ia} are energy-independent parameters occurring graphically at the vertex between channel a and particle i. Also occurring at each initial or final vertex is a form factor $f_a(s)$; for the elastic channel we use

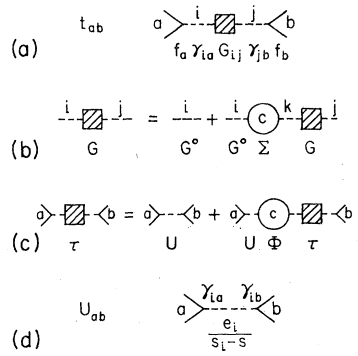

FIG. 1. (a) Graphical description of the t-matrix parametrization, Eq. (2.1). (b) The propagator Eq. (2.3). (c) The scattering Eq. (A11). (d) The effective potential (A12).

$$f_e(s)=\left(\frac{p_{\text{c.m.}}}{Q_1+(Q_2{}^2+p_{\text{c.m.}}{}^2)^{1/2}}\right)^l . \tag{2.2}$$

The other $f_a(s)$ are defined below, in Eq. (2.14). Though angular momentum and parity labels are suppressed, Eq. (2.1) parametrizes a partial-wave amplitude; l is the angular momentum in channel a, Q_1 and Q_2 are constants. The factor $f_a(s)$ provides appropriate threshold behavior on the right-hand cut, and also produces a left-hand branch cut in the s plane. Constants Q_1 and Q_2 are chosen to determine the branch point and strength of the left-hand branch cut; in our analysis they both have been set equal to the pion mass.

We assume an explicit model for the inelastic phase-space factors used in our analysis. The model is an isobarlike production model; in fact, our parametrization of $\pi N\to\pi\pi N$ scattering is similar to that used by the SLAC-Berkeley collaboration in their inelastic partial-wave analysis.[3]

The factor G_{ij} appearing in Eq. (2.1) is the dressed propagator matrix for particles i and j. It may be written in terms of a diagonal bare propagator G^0_{ij} and a self-energy matrix Σ_{lk} using the Dyson equation [see Fig. 1(b)]

$$G_{ij}=G^0_{ij}+G^0_{il}\,\Sigma_{lk}G_{kj}\,. \tag{2.3}$$

The bare propagator, with a pole at the real value s_i, is simply

$$G^0_{ij}=\frac{e_i\delta_{ij}}{s_i-s}\,. \tag{2.4}$$

The sign factor $e_i=\pm1$ must be chosen to be positive for propagators which actually correspond to

resonances, i.e., which generate poles above the elastic threshold. However, to have a simple unified formalism for treating resonances and background potentials, we simulate extra contributions to the left-hand cuts by introducing additional propagators with s_i below threshold; for these, e_i is positive to represent a repulsive potential, negative for an attractive potential. The factor Σ_{ik} in Eq. (2.3) is the self-energy term for the particle propagator:

$$\Sigma_{ik} = \sum_{a=1}^{M} \gamma_{ia} \Phi_a(s) \gamma_{ka} . \tag{2.5}$$

The $\Phi_a(s)$ are "channel propagators" which are constructed in an approximation which treats each channel as containing two particles (which may be unstable). We require that $\Phi_a(s)$ provide the correct analyticity structure for the elastic amplitude $t_{ee}(s)$, and we also require that $t_{ab}(s)$ have, in all channels, correct unitarity and analyticity properties consistent with a quasi-two-body (isobar) approximation. The imaginary part of $\Phi_a(s)$ is the effective phase-space factor for channel a.

To construct the $\Phi_a(s)$ we first define a function $\phi_{12}(s)$. This also depends on masses m_1 and m_2 and on an angular momentum l_{12}. The function $\phi_{12}(s)$ satisfies

$$\mathrm{Im}\,\phi_{12}(s) = [f_{12}(s)]^2 \rho_{12}(s) \equiv F_{12}(s) . \tag{2.6}$$

Here we use the center-of-mass momentum

$$p_{12} = \{[s-(m_1+m_2)^2][s-(m_1-m_2)^2]/4s\}^{1/2} \tag{2.7}$$

to define the two-body phase-space factor

$$\rho_{12}(s) = p_{12}/\sqrt{s} \tag{2.8}$$

and the form factor

$$f_{12}(s) = \left(\frac{p_{12}}{Q_1 + (Q_2^2 + p_{12}^2)^{1/2}} \right)^{l_{12}} . \tag{2.9}$$

The factor (2.2) used in the elastic channel is a special case of (2.9).

We construct the real part of $\phi_{12}(s)$ by using a subtracted dispersion relation

$$\phi_{12}(s) = \frac{s-s_0}{\pi} \int_{s_{12}}^{\infty} \frac{ds' \rho_{12}(s')[f_{12}(s')]^2}{(s'-s)(s'-s_0)} , \tag{2.10}$$

where $s_{12} = (m_1+m_2)^2$. We have also experimented with modifications to $\phi_{12}(s)$ which have left-hand branch cuts in addition to the right-hand unitarity cut. However, the results are essentially the same as those reported here, which are based on use of (2.10), and in which the proper left-hand cut structure is approximated by use of explicit potential terms.

In the elastic channel and the ηN channel, which are true two-body channels, we use $\Phi_a(s) = \phi_{12}(s)$, with the appropriate masses being used in the definition of ϕ_{12}. In $\pi\pi N$ quasi-two-body channels we use,

$$\Phi_a(s) = \int_{w_2^2}^{\infty} dm_2^2 \sigma_a(m_2^2) \phi_{12}(s) , \tag{2.11}$$

where $w_2 = 2m_\pi$ or $m_\pi + m_N$, depending on the isobar being considered. The resonance weighting function is

$$\sigma_a(M^2) = \frac{\gamma F_a(M^2)/\pi}{\{(R-M^2)^2 + \gamma^2 [F_a(M^2)]^2\}} , \tag{2.12}$$

where F_a is given by (2.6) and where R and γ are chosen to give the correct mass and width for the resonant quasiparticle [e.g., the $\Delta(1234)$, ρ, ϵ, ω, and $N^*(1470)$]. The poles of σ_a generate second-sheet branch cuts in $\Phi_a(s)$ starting from quasi-two-body inelastic thresholds.

We also include a nonresonant background $\pi\pi N$ channel, in which $\sigma(M^2) = p_{12}(M^2)/M^2$, where p_{12} is the πN center-of-mass momentum. In some partial waves we included a $\rho\Delta$ channel. The $\rho\Delta$-channel propagator was defined by a double integral:

$$\Phi_{\rho\Delta}(s) = \int_{4m_\pi^2}^{\infty} \sigma_\rho(m_1^2) dm_1^2 \times \int_{(m_\pi+m_N)^2}^{\infty} \sigma_\Delta(m_2^2) dm_2^2 \phi_{12}(s) , \tag{2.13}$$

where σ_ρ and σ_Δ are the same weighting functions used in (2.11). To evaluate the integrals in (2.10)–(2.13) we found it convenient to choose paths parallel to the imaginary axes.

The unitarity properties of our formalism are discussed in the appendix. The form factor f_a for channel a is defined by the relation

$$\mathrm{Im}\Phi_a = f_a^2 \rho_a \equiv F_a , \tag{2.14}$$

where ρ_a is given by (2.11) or (2.13) with ϕ_{12} replaced by ρ_{12} (which is real). A definition of effective phase-space factors which are similar to our functions $\Phi_a(s)$ has been suggested recently by Basdevant and Berger.[12] We point out that even in K-matrix fits it is necessary to include the extra integral (2.10) in discussing inelastic channels. Otherwise (as in Longacre *et al.*[3]), even the elastic amplitude will be given spurious singularities.

Not all of these phase-space factors were necessary to parametrize a single resonance. The factors included for a given resonance, or for a given partial wave, were suggested first by the channels found important in the SLAC-Berkeley[3] and Imperial College[4] single-pion production partial-wave analyses. The final criterion for the choice of channels in any partial wave was to have a good fit to the elastic partial-wave amplitudes,

and in most cases, to the inelastic partial-wave cross sections determined by the SLAC-Berkeley and Imperial College analyses.

In the partial-wave fits, we have usually used one attractive and one (occasionally two) repulsive below-threshold terms coupled to the elastic channel and generally having fixed s_i values. One resonance term was included for each resonance appearing in the tables, and also for one (sometimes two) additional "background" resonances which had their s_i values fixed at arbitrarily chosen large values above the data region. The above-threshold resonances were most commonly coupled to three inelastic channels as well as to the elastic channel, although considerable experimentation was done on the number and character of these channels in order to check the stability of the results. Readers interested in further details may contact one of the authors.

III. DEFINITION OF RESONANCE PARAMETERS

In this section resonance parameters are defined. Partial-wave resonances are economically described in single-channel analyses by a resonance mass, width, and elasticity, or by the pole position in the complex energy plane and its residue. Our coupled-channel analysis complicates the mathematical formalism, but we have sought to define parameters which may be compared directly to familiar single-channel-analysis definitions.

We begin by introducing a T matrix which has a unitary normalization

$$T_{ab}=\sqrt{\rho_a}\,t_{ab}\sqrt{\rho_b} \tag{3.1}$$

and the M-channel S matrix

$$S=1+2iT. \tag{3.2}$$

The K matrix is defined to be real, and in terms of S and T is

$$K=i\frac{1-S}{1+S}=\frac{T}{1+iT}. \tag{3.3}$$

The standard single-channel resonance parameters are often defined through a Breit-Wigner parametrization of the partial-wave amplitude:

$$T=\frac{\Gamma_e/2}{m-E-i\Gamma_{\rm tot}/2}, \tag{3.4}$$

where m is the resonance mass, Γ_e the elastic width, and $\Gamma_{\rm tot}$ the total resonance width. The elasticity of the resonance is defined by the ratio

$$x_e=\frac{\Gamma_e}{\Gamma_{\rm tot}}. \tag{3.5}$$

Complications arise from the fact that in practice Γ is energy dependent. Nearby resonances, and also more slowly varying background effects, may further distort the shape of the resonance.

A number of alternative definitions of resonance parameters have been investigated in our coupled-channel analysis. They include defining resonance parameters using the pole of the K matrix and using the pole of the T matrix. The pole of the K matrix is determined by the condition

$$\det(1+S)=\det(1+iT)=0. \tag{3.6}$$

In the vicinity of the pole, the K matrix can be parametrized as

$$K\sim\frac{\Gamma/2}{E_0-E}\chi\chi^\dagger \tag{3.7}$$

where χ represents a normalized coupling vector satisfying $\chi^\dagger\chi=1$.

A third method of defining resonance parameters is to associate resonances with poles of the T matrix. Using (2.1), (2.14), and the definition $H^{-1}\equiv G$, the T matrix can be written in the form

$$T_{ab}=\sum_{ij}\gamma_{ia}\sqrt{F_a}\;H_{ij}^{-1}\gamma_{jb}\sqrt{F_b}. \tag{3.8}$$

The condition that the matrix T_{ab} has a pole reduces, using Eq. (A9), to the condition

$$\det H_{ij}=\det[e_i\delta_{ij}(s_i-s)-\Sigma_{ij}]=0. \tag{3.9}$$

The mass m and width Γ can be defined in terms of the pole position $s_0=(m-\frac{1}{2}i\Gamma)^2$. In the vicinity of the pole we can parametrize H^{-1} in the form

$$H^{-1}{}_{ij}=\chi_i\chi_j/h(s), \tag{3.10}$$

where the coupling vector χ is an eigenvector of H at $s=s_0$:

$$\sum_j H_{ij}(s_0)\chi_j=0 \tag{3.11}$$

and where

$$\sum_{ij}\chi_i H_{ij}(s)\chi_j=h(s). \tag{3.12}$$

By use of (3.9) and (2.5) we obtain

$$h(s)=\sum_i e_i\chi_i{}^2(s_i-s)-\sum_c\eta_c{}^2\Phi_c, \tag{3.13}$$

where

$$\eta_c=\sum_i\gamma_{ic}\chi_i. \tag{3.14}$$

The η_c define the coupling of the resonance to channel c, as is clear from the expression for the residue of T_{ab}:

$$R_{ab}=(F_aF_b)^{1/2}\eta_a\eta_b/h'(s), \tag{3.15}$$

where $h' = dh/ds$. The elasticity can be defined in terms of the residue R_{ee} of the elastic amplitude. By comparison with Eq. (3.4), it is seen that $R_{ee} \approx m\Gamma_e$, so that

$$x_e = |R_{ee}|/[-\mathrm{Im}(s_0)]. \tag{3.16}$$

This prescription for identification of resonances and resonance parameters was found to be preferable to the K-matrix prescription; the results were more stable, and less dependent on M, the number of channels being parametrized. A difficulty of this method is that it is sometimes hard to interpret the results when the phase space factors are rapidly varying.

The energy dependence of the $F_a(s)$ generally displaces a pole from the conventionally accepted resonance position. Furthermore, in a multichannel formalism, a single resonance usually corresponds to several poles of T, on different sheets of the s-plane Riemann surface, depending on how the branch points of the phase-space factors are avoided in the analytic continuation from real s. We generally choose the pole reached most directly, by analytic continuation with Res fixed. In certain cases this condition is somewhat ambiguous because a strong inelastic channel opens within the width of the resonance. This occurs, for example, in the case of the first S_{11} resonance (which is strongly coupled to the ηN channel) and in the case of several resonances which are close to the ρN threshold.

The K-matrix poles are on the real axis, so the ambiguity of analytic continuation path does not arise. However, quite different results are obtained on changing the number of channels which are considered to be open.

In order to have a prescription which is simple, relatively unique, and in close correspondence with standard procedure, we use a combination of methods 1 and 3. First, we identify a resonance by locating the pole in T. Then we consider the width to be an energy-dependent quantity involving the phase-space factors:

$$\Gamma \sim \sum_c y_c F_c(s), \tag{3.17}$$

where F_c is defined in Eq. (2.14) and

$$y_c = |\eta_c|^2. \tag{3.18}$$

In the neighborhood of the resonance, we generalize the parametrization of (3.4) to

$$T_{ab} = (B_{ab} - \delta_{ab})/2i + \sum_{cd} B_{ac}{}^{1/2} F_c{}^{1/2} \eta_c D^{-1} \eta_d F_d{}^{1/2} B_{db}{}^{1/2}, \tag{3.19}$$

where B_{ab} is a background S matrix (which is assumed to be slowly varying but plays no role in the following) and where the generalized Breit-Wigner demoninator is

$$D(s) = r - s - c\sum_c y_c \Phi_c(s). \tag{3.20}$$

The real constants r and c are chosen so that $D(s_0) = 0$. Note that $D(s)$ would be proportional to $h(s)$ if all of the χ_l, and hence all of the η_c, would have the same phase. Although this is not generally true, if s_0 is close to a branch point of some $\Phi_c(s)$, we expect that the zeros of $D(s)$ on the other sheets will still give an adequate approximation to the entire set of poles of T_{ab} which are associated with the resonance.

We define the mass m of the resonance by

$$\mathrm{Re}D(m^2) = 0 \tag{3.21}$$

and the width by

$$\Gamma = \mathrm{Im}D(m^2)/[m\,\mathrm{Re}D'(m^2)]. \tag{3.22}$$

We interpret the quantity

$$\Gamma_c = \frac{y_c F_c(m^2)\Gamma}{\sum_a y_a F_a(m^2)} \equiv x_c \Gamma \tag{3.23}$$

as the partial width in channel c, and the quantity x_e, in particular, as the elasticity. The quantities listed in Tables I and II were obtained by the use of Eqs. (3.21)–(3.23).

IV. PARTIAL-WAVE AMPLITUDES AND RESONANCE PARAMETERS

Figures 2–6 exhibit the partial-wave amplitudes from the preceding paper[1] along with the parametrizations obtained by maximum-likelihood fits to the partial-wave and inelasticity data. The elastic-channel amplitudes and some inelastic cross sections were fitted using the multichannel formalism described in Sec. II. The partial-wave amplitudes of Ref. 1 were augmented by lower-energy results from Bugg[10] and higher-energy results from Ayed.[6]

The Bugg amplitudes, for $L \leq 3$ (except F_{17} and F_{35}) at 9 momenta with $P_{\mathrm{lab}} \leq 0.408$ GeV/c, were reasonably continuous with our partial waves. For the partial waves neglected by Bugg, the amplitudes shown in Figs. 2–6 are in fact very small for $P_{\mathrm{lab}} \leq 0.6$ GeV/c. We used partial-wave amplitudes from Ayed at 6 momenta above 2.0 GeV/c, for those partial waves in which there was adequate continuity. Generally speaking, the partial waves with $\frac{5}{2} \leq J \leq \frac{11}{2}$ matched ours reasonably well at 2.0 GeV/c, while other partial waves did not. The errors on the high-energy amplitudes taken from Ayed were enlarged to make the statistical weights of those data comparable to the

TABLE I. Even-parity states. Asterisks indicate status rating based on previous analyses.[15] The letters A, F, C have the following significance. A: Alternate fits containing an additional resonance are possible. F: The fit does not adequately describe the observed structure. This might be an indication that additional resonances are present, but satisfactory fits with an additional resonance have not been obtained. C: The parameters of this resonance depend on continuity with the results of Ref. 6. Consistent error estimates are not possible. B is the brightness parameter (see text).

States $L_{2I,2J}$	Mass (MeV)	Width (MeV)	Elasticity x	$SU_6 \times O_3$	Notes	B
P_{31}	1920 ± 50	300 ± 100	0.19 ± 0.04	[56, 2^+]	**** A	3.2
$P_{33}(1)$	1234	124	1.00	[56, 0^+]	****	0
$P_{33}(2)$	1640 ± 50	370 ± 70	0.20 ± 0.04	[56, 0^+]*	***	2.5
$P_{33}(3)$	1960 ± 80	300 ± 100	0.17 ± 0.04	[56, 2^+]	F	3.0
F_{35}	1920 ± 30	340 ± 80	0.15 ± 0.02	[56, 2^+]	**** F	2.8
F_{37}	1950 ± 20	340 ± 60	0.40 ± 0.02	[56, 2^+]	****	1.7
$P_{11}(1)$	938	...	...	[56, 0^+]	****	...
$P_{11}(2)$	1450 ± 30	370 ± 80	0.65 ± 0.05	[56, 0^+]*	**** F	1.6
$P_{11}(3)$	1710 ± 60	100 ± 50	0.19 ± 0.05	[70, 0^+]	*** F	3.2
P_{13}	1740 ± 80	210 ± 80	0.19 ± 0.05	[56, 2^+]	*** A	2.9
F_{15}	1680 ± 15	120 ± 25	0.62 ± 0.06	[56, 2^+]	**** A	1.4
F_{17}	1970 ± 80	325 ± 150	0.06 ± 0.02	[70, 2^+]	** A	3.9
H_{19}	(2250)	(450)	(0.02)	[56, 4^+]	*** C	2.8

weights of the data at momenta just below 2 GeV/c.

It has generally been quite hard to fit the inelasticity data[3,4] in conjunction with the elastic amplitudes. We have usually ended up using the inelasticity data only qualitatively, and we note here two points where there are difficulties even at the qualitative level. Our D_{33} amplitude becomes nearly elastic near 1900 MeV, and is similar to the Helsinki-Karlsruhe (HK) (Ref. 5) amplitude in this respect. However, the inelasticity reported in Ref. 3 does not have such a dip, but remains significantly greater. Secondly, although the HK analysis reports different D_{35} resonance parameters than we do, there is agreement between us and also with Ayed[6] that this partial wave does have significant inelasticity above 1800 MeV; our disagreement arises, in part, from the fact that the HK inelasticity does not have a dip around 2000 MeV. The inelasticity data cannot help to resolve this question because

TABLE II. Odd-parity states. The notes have the same meaning as in Table I.

States $L_{2I,2J}$	Mass (MeV)	Width (MeV)	Elasticity x	$SU_6 \times O_3$	Notes	B
$S_{31}(1)$	1620 ± 20	140 ± 20	0.25 ± 0.04	[70, 1^-]	****	2.6
$S_{31}(2)$	1850 ± 35	130 ± 40	0.08 ± 0.03	[56, 1^-]	*	4.0
$S_{31}(3)$	2150 ± 100	230 ± 80	0.10 ± 0.04	[70, 1^-]*		4.0
$D_{33}(1)$	1730 ± 30	300 ± 100	0.12 ± 0.04	[70, 1^-]	***	3.1
$D_{33}(2)$	2010 ± 100	240 ± 60	0.05 ± 0.02	[56, 1^-]		4.3
D_{35}	1930 ± 20	280 ± 90	0.12 ± 0.03	[56, 1^-]	***	3.1
G_{37}	(2200)	(350)	(0.05)	[70, 3^-]	C	4.0
$S_{11}(1)$	1540 ± 20	270 ± 50	0.45 ± 0.06	[70, 1^-]	****	2.1
$S_{11}(2)$	1640 ± 30	140 ± 40	0.60 ± 0.05	[70, 1^-]	****	1.9
$D_{13}(1)$	1525 ± 15	125 ± 25	0.56 ± 0.06	[70, 1^-]	****	1.5
$D_{13}(2)$	1670 ± 25	80 ± 40	0.10 ± 0.02	[70, 1^-]	***	3.4
$D_{13}(3)$	1830 ± 50	125 ± 50	0.06 ± 0.03	[56, 1^-]		4.1
$D_{13}(4)$	2100 ± 80	300 ± 100	0.13 ± 0.05	[70, 3^-]	**	3.6
D_{15}	1680 ± 15	180 ± 30	0.35 ± 0.06	[70, 1^-]	****	2.0
G_{17}	2150 ± 100	300 ± 100	0.16 ± 0.07	[70, 3^-]	*** AC	3.0
G_{19}	(2200)	(330)	(0.10)	[70, 3^-]	*** C	3.4

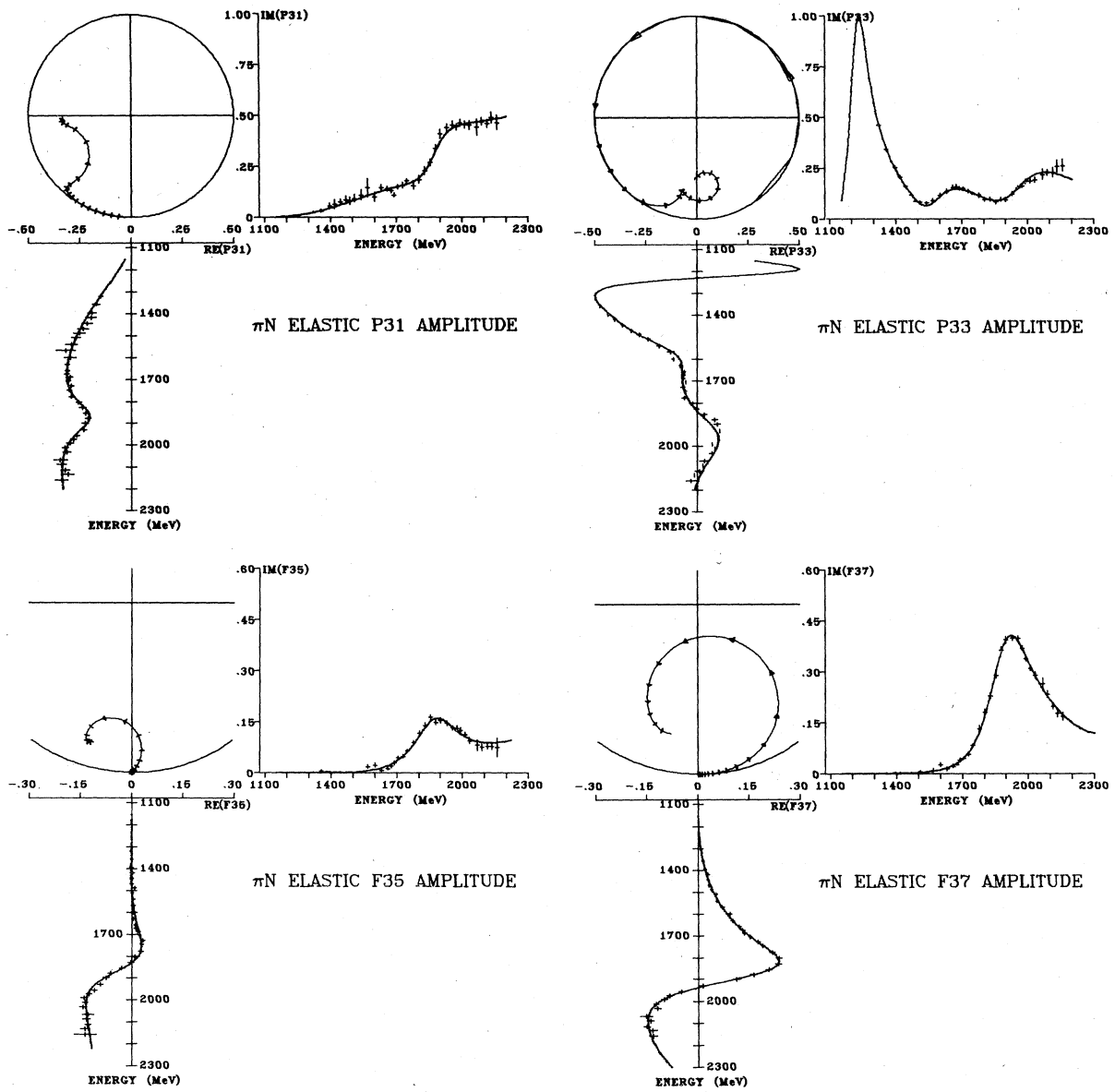

FIG. 2. Even-parity $I=\frac{3}{2}$ partial-wave amplitudes for $J\leq\frac{7}{2}$. The data points for real and imaginary parts are the results from Ref. 1. The curves show fits obtained by the method described in the text. On the projections of fits onto the Argand plots, the energy dependence is indicated by arrows which have bases at multiples of 50 MeV and a base-to-tip length of 5 MeV.

the D_{35} amplitudes were omitted in the SLAC-Berkeley analysis.[3]

Data on the magnitude[13] and phase[14] of the ηn threshold production amplitude were used in fits to the S_{11} partial wave.

Estimation of errors in partial-wave analysis is very hard, and a great deal of attention was given to this problem in Ref. 1. One aspect of this problem which is especially hard to treat is that the errors do not have a Gaussian character. This arises in part from propagation of non-Gaussian errors in the data, and in part from the nonlinear nature of the energy-dependent partial-wave fitting. Since the fitted observables are complicated nonlinear functions of the partial-wave amplitudes, the likelihood function is only roughly approximated by a Gaussian function. In fitting the derived partial-wave amplitudes as a function of energy, we attempt to take this into account by modifying the χ^2 function.

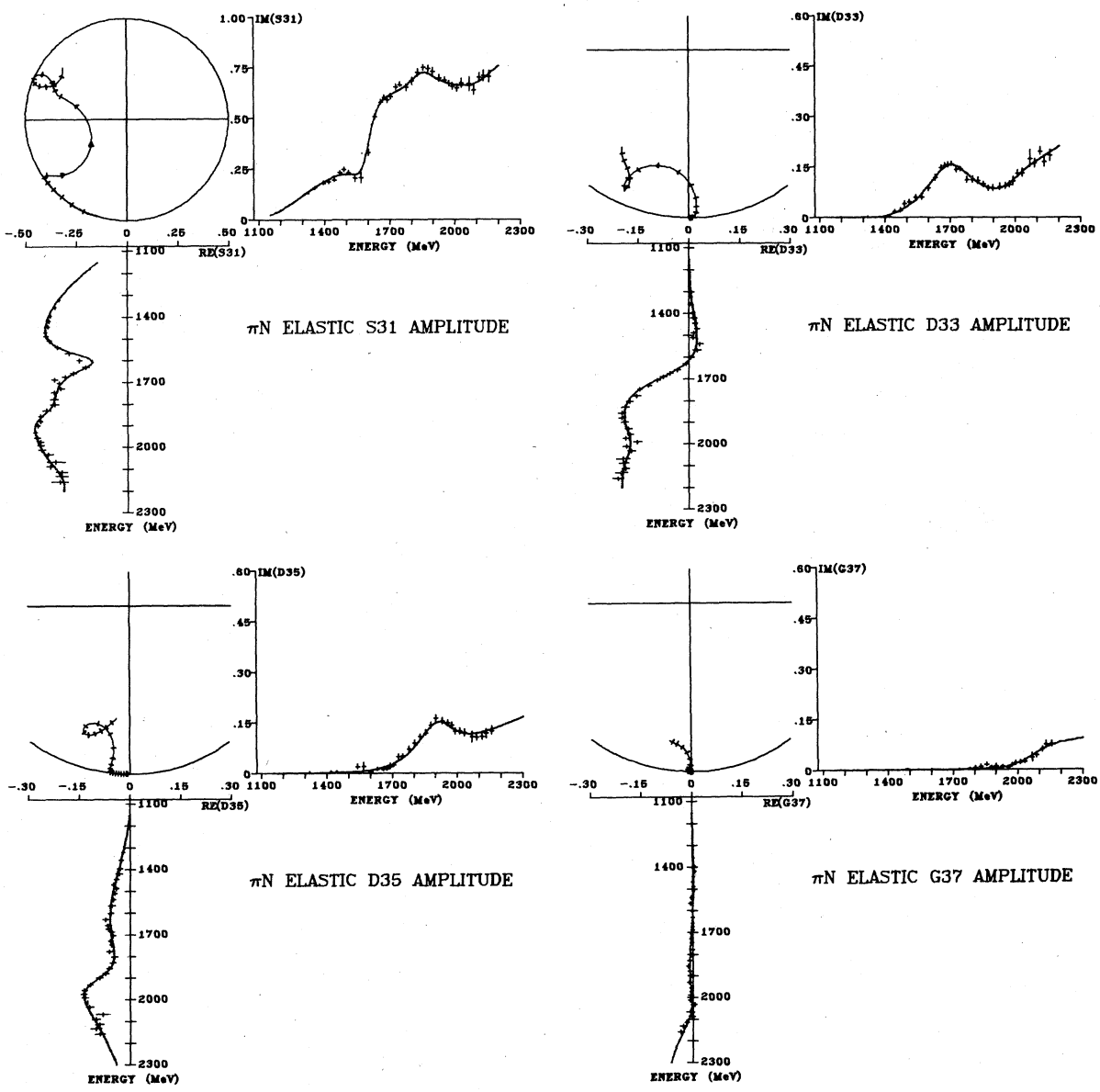

FIG. 3. Odd-parity $I=\frac{3}{2}$ partial-wave amplitudes for $J\leq\frac{7}{2}$. See also the caption to Fig. 2.

We denote the usual χ^2 contribution from the data on a given channel amplitude at a given energy by

$$\Delta^2=\sum_{i,j=1}^{n}(D_i-F_i)W_{ij}(D_j-F_j)\,, \tag{4.1}$$

where D_i are the data, F_i the parametrized fit, and W is the weight matrix. Here i and j have a range $n=2$ when we consider the real and imaginary parts of the elastic amplitude at energies where the inelasticity is non-negligible. Otherwise, for the elastic amplitude at very low energies, or for the inelastic cross sections for specific channels, their range is $n=1$. We replace the conventional χ^2 function (which is just the sum of Δ^2 over channels and energies) by modifying the likelihood function $\mathcal{L}$ to allow for longer tails than are given by a Gaussian:

$$-2\ln[\mathcal{L}(\text{per energy, channel})]=\overline{\Delta}^2\,, \tag{4.2}$$

where, for $\Delta^2<\Delta_0^2$,

$$\overline{\Delta}^2=\Delta^2 \tag{4.3a}$$

and otherwise

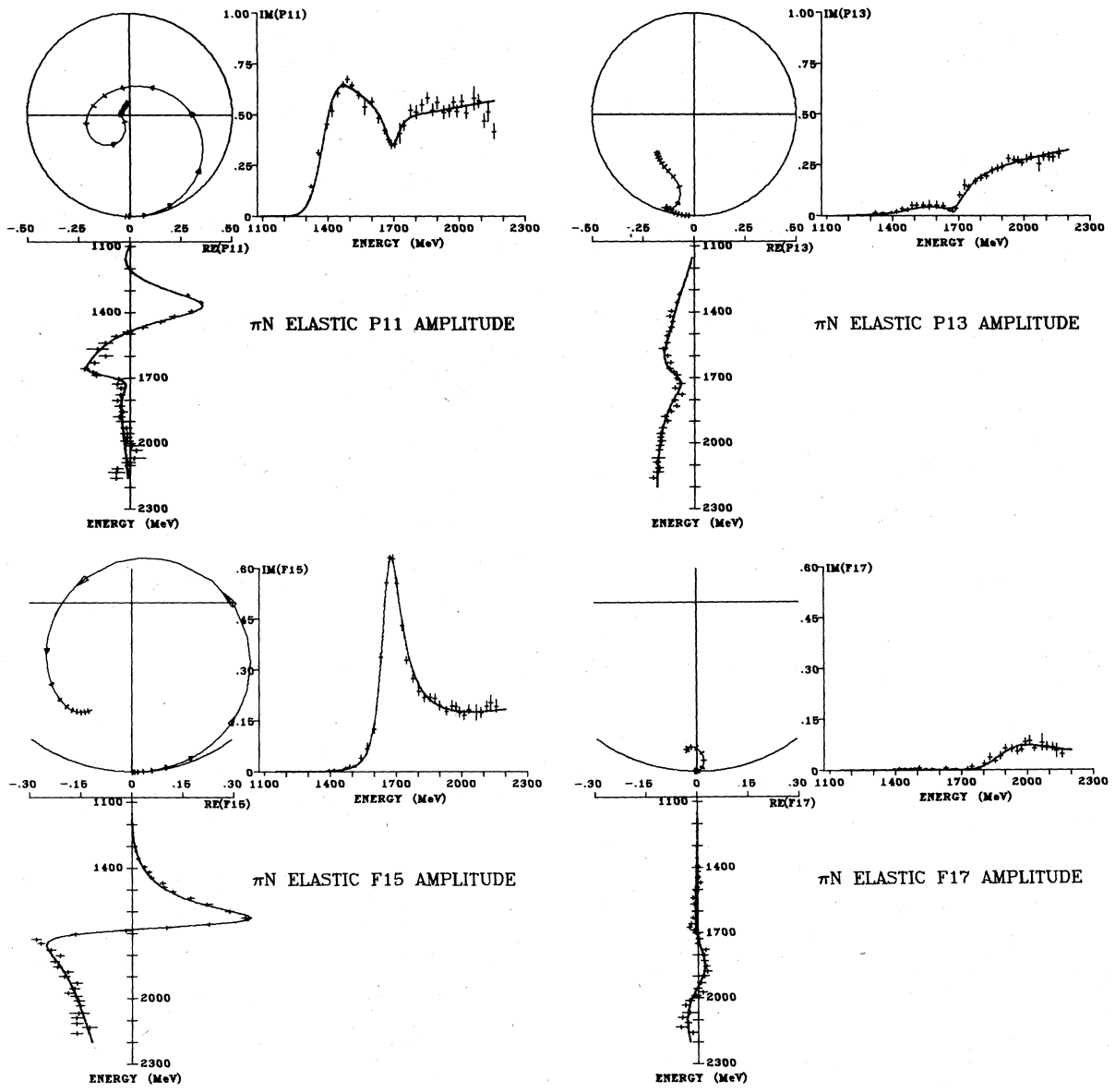

FIG. 4. Even-parity $I=\frac{1}{2}$ partial-wave amplitudes for $J\leq\frac{7}{2}$. See also the caption to Fig. 2.

$$\overline{\Delta}^2=\Delta_0{}^2+\ln(1+\Delta^2-\Delta_0{}^2)+\tfrac{1}{2}[\ln(1+\Delta^2-\Delta_0{}^2)]^2\,. \tag{4.3b}$$

The transition value is taken to be

$$\Delta_0{}^2=2n\frac{N-\nu}{N}\,, \tag{4.4}$$

where N is the total number of data and ν is the number of parameters.

The form used in Eqs. (4.2)–(4.4) has been chosen to have the following properties, which are easily verified. The modified likelihood function has continuous first and second derivatives with respect to the F_i at the point where $\Delta^2=\Delta_0{}^2$. All positive moments of Δ^2 have finite expectation values. The correction (4.3b) is applied only if the confidence level is below about 15%, and it is important only if the confidence level falls below a few percent. Since this modification affects only about 15% of the data, the modified χ^2 function is not significantly harder to calculate.

Tables I and II list the resonances and resonance parameters determined by Eqs. (3.21)–(3.23). For the P waves and for F_{15} and G_{17}, the tables

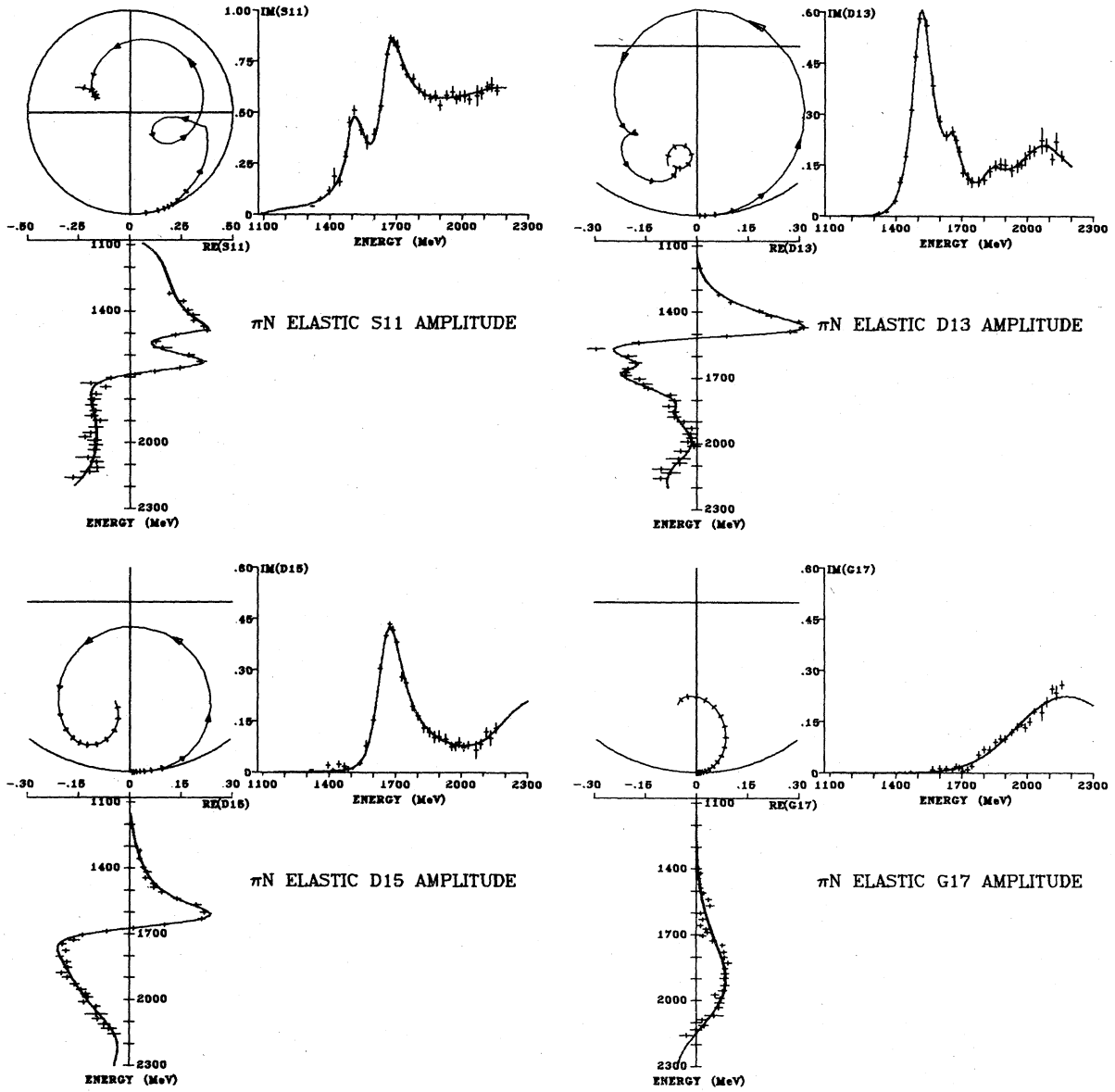

FIG. 5. Odd-parity $I=\frac{1}{2}$ partial-wave amplitudes for $J\leq\frac{7}{2}$. See also the caption to Fig. 2.

list only preliminary results. Additional structure may also be present. For the other partial waves, all the resonant structure for which we have evidence has been tabulated.

The uncertainties on resonance parameters listed in the two tables are somewhat subjective. We have combined the range of values obtained with different parametrizations with previous estimates from a Monte Carlo procedure. In Ref. 11, we varied partial-wave amplitudes within Gaussian distributions determined by the partial-wave uncertainties, and then refitted. We have scaled these estimates in accordance with the size of the errors on the partial-wave amplitudes in the resonance region.

The S_{11} and P_{11} partial waves are both quite erratic, especially above 1800 MeV, and are also highly correlated with each other. In the fit to the P_{11} partial wave, shown in Fig. 4, we found resonances at 1450 and 1710 MeV. However, since the fit is quite poor, we are not able to estimate errors reliably, and we do not know whether other meaningful structure might be present. In the P_{31}, P_{13}, F_{15}, and G_{17} partial waves, in addition to

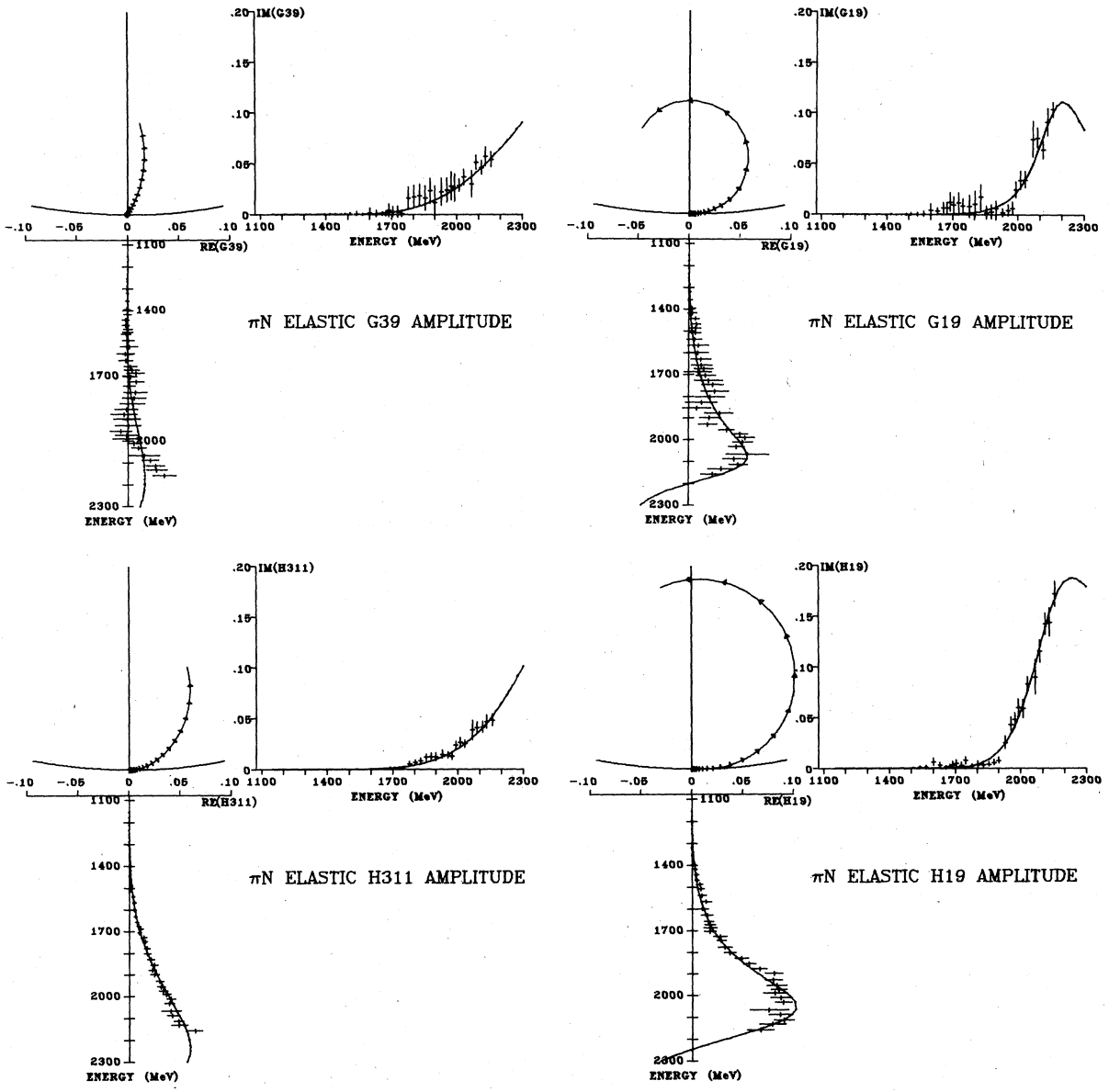

FIG. 6. Amplitudes for peripheral partial waves which have resonances just above the energy region analyzed in Ref. 1. The fits include data from Ref. 6 above 2190 MeV. See also the caption to Fig. 2.

the fits shown, we also have fits (with substantially decreased χ^2) in which the listed resonances are accompanied by other, weaker resonances. In these two-resonance fits, the parameters of the stronger resonance are somewhat altered. Further analysis is required for resolution of the structure in these partial waves.

The fit in the third P_{33} resonance region is not good and the parameters are not well determined. In the D_{33} partial wave, the parameters of the two resonances are especially uncertain because the two resonances seem to interfere in such a way that the width of the first and the mass of the second are highly correlated.

Tables I and II also list several other features of observed resonances. One column gives a conjectured $SU_6 \times O_3$ multiplet assignment for each resonance. Some of these assignments are quite speculative, and should be considered to be primarily a means of comparing the number of observed resonances with the number expected in various models. As a guide to the difficulty of identifying resonance states, we give for each resonance a brightness or magnitude parameter

defined to be

$$B = B_0 - \ln \left| \frac{x}{P_{\text{c.m.}}} (2J+1)^{1/2}(2I+5)^{1/2} \right| , \qquad (4.5)$$

with B_0 chosen to fix the normalization so that $B = 0$ for the $\Delta(1234)$ resonance. The argument of the logarithm represents an average contribution of the resonance to the $\pi^{\pm}p$ elastic and charge-exchange amplitudes. As for stellar magnitudes, a larger magnitude B corresponds to a fainter resonance, a resonance which is necessarily more uncertain.

Finally, a number of comments appear in the tables. For resonances which have appeared in other analyses, we list the status rating of the resonance, as it appears in the Review of Particle Properties.[15] The effect our own analysis might have on the status rating has not been taken into account. Notes *A* or *F* attached to a resonance indicate that additional structure may be present in the partial wave, but the partial-wave data do not permit resolution of the structure at this time. Note *C* indicates that only a portion (usually the lower half) of the resonance falls within our partial-wave data; in such cases our data are reasonably continuous with the higher-energy partial-wave data of Ayed,[6] and we have relied on those higher-energy points to some extent in determining resonance parameters.

Table III lists the pole positions and residues for each of the resonances appearing in Tables I and II.

The resonance shapes are modified, in some cases quite strongly, by low-energy background terms in the fits. These background effects have characteristic regularities which are apparent in Figs. 2–6. The low-energy background for partial waves with $j = 2k + 1 + n/2$ for a given $n = \pm 1$ and a given isospin I and parity P has similar properties for $k = 0$, 1, and 2. (Only half of the $k = 2$ partial waves are shown in Fig. 6.) For $n = -1$, $P = \pm 1$, there is attraction for $I = \frac{1}{2}$ and a strong repulsion for $I = \frac{3}{2}$. For $n = +1$, there is attraction for $I = \frac{3}{2}$, $P = +1$ and $I = \frac{1}{2}$, $P = -1$, and repulsion for $I = \frac{3}{2}$, $P = -1$ and $I = \frac{1}{2}$, $P = +1$. Effects of this general nature are to be expected on the basis of long-range forces arising from meson and baryon exchange. Baryon exchange is responsible for the dependence on n. At low energies the dominant contribution is expected to be given by nucleon and $\Delta(1234$ MeV) exchange, and to be more important for even parity than for odd parity, as is observed.

The input partial-wave data from Ref. 2 may be obtained on magnetic tape from R.L.K.

V. DISCUSSION

As can be seen from Tables I and II, our analysis provides new determinations of parameters for a number of well-established baryon resonances. In addition, we find some evidence for several states which were quite speculative or nonexistent in previous analyses. These include a second S_{31}

TABLE III. Pole positions and residues.

Odd-parity states			Even-parity states		
State	Pole position (MeV)	Residue (MeV)	State	Pole position (MeV)	Residue (MeV)
$S_{31}(1)$	$1597 - 60i$	$-6 - 15i$	P_{31}	$1871 - 100i$	$-0.6 - 18i$
$S_{31}(2)$	$1844 - 71i$	$7 - 1i$			
$S_{31}(3)$	$2135 - 134i$	$-9 - 13i$			
$D_{33}(1)$	$1691 - 146i$	$24 - 2i$	$P_{33}(1)$	$1209 - 50i$	$35 - 38i$
$D_{33}(2)$	$1997 - 115i$	$-0.3 - 5i$	$P_{33}(2)$	$1547 - 115i$	$-18 - 11i$
			$P_{33}(3)$	$1933 - 140i$	$-10 - 27i$
D_{35}	$1908 - 113i$	$13 + 2i$	F_{35}	$1865 - 133i$	$20 - 5i$
G_{37}	$2094 - 147i$	$2 - 7i$	F_{37}	$1892 - 124i$	$43 - 24i$
$S_{11}(1)$	$1465 - 128i$	$48 - 67i$	$P_{11}(2)$	$1369 - 89i$	$-9 - 48i$
$S_{11}(2)$	$1639 - 70i$	$3 - 58i$	$P_{11}(3)$	$1692 - 44i$	$-9 + 0.1i$
$D_{13}(1)$	$1510 - 57i$	$34 - 8i$	P_{13}	$1702 - 79i$	$-6 - 8i$
$D_{13}(2)$	$1660 - 38i$	$4 - 0.3i$			
$D_{13}(3)$	$1818 - 61i$	$3 - 3i$			
$D_{13}(4)$	$2053 - 154i$	$24 - 10i$			
D_{15}	$1663 - 75i$	$33 - 11i$	F_{15}	$1666 - 56i$	$31 - 15i$
G_{17}	$2111 - 154i$	$24 - 12i$	F_{17}	$1899 - 104i$	$3 - 6i$
G_{19}	$2169 - 145i$	$15 - 7i$	H_{19}	$2180 - 200i$	$37 - 21i$

state at 1850 MeV, a second D_{33} at 2010 MeV, third and fourth D_{13} states at 1830 and 2100 MeV, and possibly a $G_{37}(2200)$ state.

In regard to the $SU_6 \times O_3$ classification of resonances, we find the nonstrange members of a number of multiplets. We observe candidates for all the expected nonstrange members of the $[56, 0^+]$*, $[70, 1^-]$, and $[56, 2^+]$ multiplets. We observe a strong $D_{35}(1930)$ resonance, which is attributed to the nonminimal $[56, 1^-]$ multiplet, and we also find somewhat weaker evidence for $D_{13}(1830)$, $S_{31}(1850)$, and $D_{33}(2010)$ states consistent with this multiplet. The statistical significance of these three resonances is not high, about three standard deviations or perhaps even less. Unlike some weak resonances found in fits to even-parity partial waves, these resonances do not lie near other stronger resonances or strong inelastic thresholds. Thus, the interpretation of the fits is not confused by overlap with other structure. We have many members of the $[70, 3^-]$ multiplet, but these states above 2050 MeV depend on using the older results of Ayed[6] in conjunction with the amplitudes from Ref. 1.

The recent HK (Ref. 5) analysis, which also made extensive use of analyticity properties, has reported resonances with masses up to 3 GeV. The forms of the analyticity constraints used by HK were substantially different, as were the treatment of the experimental data and the methods used to identify resonances and determine their parameters, so a detailed comparison with these results is of interest. Both the HK analysis and our analysis report a clear resonant structure in the F_{17} partial wave near 2 GeV, which could be attributed to the $[70, 2^+]$ multiplet of $SU_6 \times O_3$. Their S_{31} amplitudes below 2 GeV are similar to ours, and they also identify a second resonance as a component of $[56, 1^-]$. We agree on the properties of the previously known 4* resonances, and in the G and H waves where HK find masses in the range 2.2–2.5 GeV, our amplitudes are consistent with the low-energy sides of these resonances.

In those partial waves ($F_{15}, P_{13}, P_{31}, G_{17}$) in which we may have some evidence for additional structure, the HK amplitudes are qualitatively quite similar to ours. A second resonance was reported in the F_{15} partial wave by HK, but not in the other three partial waves.

There are substantial differences in the D_{35}, D_{13}, and P_{33} waves. HK also have a D_{35} resonance near 1930 MeV, assigned to $[56, 1^-]$, but with a much smaller elasticity. In the D_{13} partial wave, the parameters of the second resonance are different, and HK do not report a third. In the P_{33} partial wave, the parameters of the second resonance near 1640 MeV are different, but there is again rough agreement around 1900–2000 MeV, where a third resonance occurs.

There are somewhat smaller differences in the remaining amplitudes. HK do not report a second D_{33} resonance, but do report a third S_{11} resonance at 1880 MeV $[56, 1^-]$ and a third P_{11} resonance at 2050 MeV $[70, 2^+]$.

In summary, we have reported the resonance structure and resonance parameters for the unambiguous partial waves in a pion-nucleon partial-wave analysis between 0.42 and 2.0 GeV/c pion laboratory momentum. Our results, for states usually attributed to even-parity 56-plets or to odd-parity 70-plets, are in general agreement with previous results. In addition, there is substantial evidence for an odd-parity 56-plet. There are P_{11} and F_{17} resonances which can be accommodated most easily in even-parity 70-plets. Further study is needed to clarify certain other even-parity partial waves which might have states associated with 70-plets.

ACKNOWLEDGMENTS

We thank Ramesh Bhandari for discussions of the ηn-threshold data and for assisting with the ηn threshold in our computer code for the S_{11} amplitude. This work was supported, in part, by the Division of High Energy Physics of the U. S. Department of Energy under Contracts Nos. EY-76-02-3066 and W-7405-ENG-48, and by the Elementary Particle Physics Program of the U. S. National Science Foundation under Grant No. PHY76-21097.

APPENDIX: PROPERTIES OF THE RESONANCE PARAMETRIZATION

In this section, we first show that the scattering matrix for t_{ab} defined by Eq. (2.1) satisfies the unitarity condition

$$\mathrm{Im}t_{ab} = \sum_c t^*_{ac} \rho_c t_{cb} , \tag{A1}$$

ρ_c being the phase space for channel c. We begin by replacing Eq. (2.1) by

$$t_{ab} = f_a \gamma^\dagger_{ai} H^{-1}{}_{ij} \gamma_{jb} f_b . \tag{A2}$$

The summation convention is used here for repeated particle labels. Using $H^{-1} = G$ and the identity $\mathrm{Im}H^{-1} = (i/2)(H^{-1*} - H^{-1})$,

$$\mathrm{Im}t_{ab} = -f_a \gamma^\dagger_{ai} (H^{-1})^*_{il} (\mathrm{Im}H)_{lk} (H^{-1})_{kj} \gamma_{jb} f_b . \tag{A3}$$

With the identity $\mathrm{Im}H = -\mathrm{Im}\Sigma = -\gamma_c f_c^2 \rho_c \gamma^\dagger_c$ we get

$$\mathrm{Im}t_{ab} = \sum_c f_a \gamma^\dagger_{ai} (H^{-1})^*_{il} \gamma_{lc} f_c \rho_c f_c \gamma^\dagger_{ck} (H^{-1})_{kj} \gamma_{jb} f_b , \tag{A4}$$

or

$$\mathrm{Im}t_{ab} = \sum_c t^*_{ac}\rho_c t_{cb}. \tag{A5}$$

The Dyson equation (2.3) for the dressed propagator may be written, suppressing matrix indices, as

$$G = G^0 + G^0\Sigma G \tag{A6}$$

or

$$(G^0)^{-1} = G^{-1} + \Sigma. \tag{A7}$$

Defining the inverses

$$H = G^{-1} \text{ and } H^0 = (G^0)^{-1} = e_i\delta_{ij}(s_i - s), \tag{A8}$$

Eq. (A7) becomes

$$H = H^0 - \Sigma. \tag{A9}$$

The matrices H, G, H^0, and G^0 are $N\times N$ dimensional matrices.

Let us define τ_{ab} to be the matrix element t_{ab} with the coupling factors in Eq. (2.1) removed:

$$t_{ab} = f_a\tau_{ab}f_b. \tag{A10}$$

Then τ_{ab} also satisfies the equation, shown schematically in Fig. 1(c),

$$\tau_{ab} = U_{ab} + U_{ac}\Phi_c\tau_{cb}, \tag{A11}$$

where U_{ab} is the potential connecting channels a and b [Fig. 1(d)]:

$$U_{ab} = \sum_{ij}\gamma_{ia}\frac{e_i\delta_{ij}}{s_i - s}\gamma_{jb}. \tag{A12}$$

With this potential the elastic partial-wave amplitude would have only a right-hand cut, except that poles below threshold can approximate the properties of a left-hand cut.

In fitting the data in an energy region which contains one or two resonances, it is often computationally convenient to determine separately and treat as a fixed background the terms which correspond either to distant resonances or to potentials (left-hand cuts). This is done by separating the matrices G^0, H^0, G, and H into submatrices with n or m $(n+m=N)$ rows and columns. We continue to use G, H, etc., to refer to the $n\times n$ submatrices, and denote by A and E the $m\times m$ remaining diagonal submatrices of the original H and G, respectively, and by B and F their respective $m\times n$ off-diagonal submatrices. We denote by β the $M\times m$ submatrix of the coupling matrix γ.

The previous condition $H = G^{-1}$ now gives a set of four matrix equations which can be solved in terms of the submatrices giving

$$G = (H - B^\dagger A^{-1}B)^{-1} \equiv (\tilde{H})^{-1}, \tag{A13}$$

where

$$A = e_h(s_h - s) - \sum_c \beta_c\Phi_c\beta_c^\dagger \tag{A14}$$

and

$$B = -\sum_c \beta_c\Phi_c\gamma_c^\dagger. \tag{A15}$$

The definition of the self-energy matrix in the coupled channel case may be extended in the same manner:

$$\Sigma \to \tilde{\Sigma} = \Sigma + B^\dagger A^{-1}B. \tag{A16}$$

Thus, the extended Dyson equation becomes

$$\tilde{H} = H^0 - \tilde{\Sigma}. \tag{A17}$$

The coupled-channel scattering matrix now may be written

$$t_{ab} = f_a(\gamma_a^\dagger G\gamma_b + \beta_a^\dagger F\gamma_b + \gamma_a^\dagger F^\dagger\beta_b + \beta_a^\dagger E\beta_b)f_b. \tag{A18}$$

By defining new (energy-dependent) coupling constants

$$\tilde{\gamma}_b = \gamma_b - B^\dagger A^{-1}\beta_b = \gamma_b + \sum_c \gamma_c\Phi_c\beta_c^\dagger A^{-1}\beta_b, \tag{A19}$$

Eq. (A18) becomes

$$t_{ab} = f_a\tilde{\gamma}_a^\dagger G\tilde{\gamma}_b f_b + f_a\beta_a^\dagger A^{-1}\beta_b f_b. \tag{A20}$$

The first term in Eq. (A20) is the resonant part of the scattering amplitude; the second term is a unitary background contribution to the scattering amplitude. The factors appearing in the background amplitude include the same phase-space factors Φ_c as the resonant amplitude, as well as similar propagators. These background terms are thus ensured of having proper threshold and analyticity properties. By choosing the propagator parameters s_h outside the region of the resonances under consideration, the background terms are made to be smoothly varying.

---

*Now at St. Bonaventure University, St. Bonaventure, N. Y. 14778.

[1]R. E. Cutkosky *et al.*, preceding paper, Phys. Rev. D 20, 2804 (1979).

[2]R. L. Kelly and R. E. Cutkosky, Phys. Rev. D 20, 2782 (1979).

[3]D. J. Herndon *et al.*, Phys. Rev. D 11, 3165 (1975); 11, 3183 (1975); R. L. Longacre *et al.*, *ibid.* 17, 1795 (1978).

[4]K. W. J. Barnham, in *Proceedings of the Topical Conference on Baryon Resonances*, edited by R. T. Ross and D. H. Saxon (Oxford, Univ. Press, London, 1976),

p. 109; and private communication.
[5]G. Höhler *et al.*, *Handbook of Pion-Nucleon Scattering* (Fachinformationszentrum Energie, Physik, Mathematik. Karlsruhe, 1979). Physik Daten Vol. 12-7; E. Pietarinen, Helsinki University Report No. HV-TFT-78-23, 1978 (unpublished).
[6]R. Ayed, University of Paris-Sud thesis, Report No. CEA-N-1921, 1976 (unpublished); and private communication to the Particle Data Group.
[7]S. Almehed and C. Lovelace, Nucl. Phys. B21, 157 (1972).
[8]A. T. Davies, Nucl. Phys. B21, 359 (1970).
[9]V. D. Zidell *et al.*, Phys. Rev. D (to be published).
[10]D. V. Bugg, private communication.
[11]R. E. Cutkosky *et al.*, Phys. Rev. Lett. 37, 645 (1976); R. E. Cutkosky *et al.*, in *Proceedings of the Topical Conference on Baryon Resonances*, edited by R. T. Ross and D. H. Saxon (Oxford Univ. Press, London, 1976), p. 48.
[12]J.-L. Basdevant and E. L. Berger, Phys. Rev. D 19, 239 (1979).
[13]D. M. Binnie *et al.*, Phys. Rev. D 8, 2789 (1973).
[14]R. Bhandari and Y.-A. Chao, Phys. Rev. D 15, 192 (1977).
[15]Particle Data Group, Phys. Lett. 75B, 1 (1978).